

# QCD AT HIGH TEMPERATURES AND FINITE DENSITIES: HEAVY-ION COLLISIONS\*

FEDERICA FABIANO

on behalf of the LHCb Collaboration

Università degli Studi di Cagliari, Cagliari, Italy  
and

INFN Sezione di Cagliari, Cagliari, Italy  
`federica.fabiano@cern.ch`

*Received 13 February 2023, accepted 24 August 2023,  
published online 27 October 2023*

The LHCb Collaboration pursues a full physics program studying dense QCD with both beam–beam and fixed-target collisions. In this contribution, we present the recent LHCb results including quarkonia production in peripheral and ultra-peripheral heavy-ion (HI) collisions, antiproton, and charm production in fixed-target collisions.

DOI:10.5506/APhysPolBSupp.16.8-A11

## 1. Introduction

The LHCb detector is a single-arm forward spectrometer with a unique coverage in pseudorapidity,  $2 < \eta < 5$ , with respect to other LHC experiments [1, 2]. The detector includes a high-precision tracking system providing optimal vertex and momentum resolution, two ring-imaging Cherenkov detectors for charged particle identification, a calorimeter system to identify photons, electrons and hadrons, and a muon system. The LHCb fixed-target system, called SMOG (System for Measuring the Overlap with Gas), allows for injecting a low flow rate of noble gas into the primary LHC vacuum, and studying beam–gas collisions at different nucleon–nucleon centre-of-mass (c.m.) energies,  $\sqrt{s_{NN}}$ .

The LHCb has collected a wide variety of HI and fixed-target data in recent years. In the standard collision mode, lead–lead (PbPb) data have been acquired at  $\sqrt{s_{NN}} = 5.02$  TeV with 60–100% centrality range in the LHC Run 2 (2015–2018), limited by the hardware saturation due to the high track density in the forward region. In the fixed-target configuration,

---

\* Presented at *Excited QCD 2022*, Sicily, Italy, 23–29 October, 2022.

several samples of beam–gas collisions were acquired from 2015 to 2018 at  $\sqrt{s_{NN}} = 69, 110$  GeV. These energies are higher compared to previous fixed-target experiments, but below the top RHIC energy for AA collisions.

## 2. PbPb collisions results

### 2.1. $\Lambda_c^+$ -to- $D^0$ production cross-section ratio in peripheral PbPb collisions

Heavy flavour hadrons are an optimal tool to study hadronization, in particular with baryon-to-meson production ratios. The hadronization of the  $c$ -quark has been studied here, considering the  $\Lambda_c^+$ -to- $D^0$  ratio in peripheral PbPb collisions at  $\sqrt{s_{NN}} = 5.02$  TeV [3]. The two particles have been reconstructed via the  $\Lambda_c^+ \rightarrow pK^-\pi^+$  and  $D^0 \rightarrow K^-\pi^+$  decay processes. The results for the  $\Lambda_c^+$ -to- $D^0$  cross-section ratio are reported as a function of the transverse momentum in Fig. 1 and compared both to theoretical models (left) and to a previous  $p$ Pb LHCb measurement at  $\sqrt{s_{NN}} = 5.02$  TeV (right) [4]. Considering the colour recombination mechanism, data are sufficiently well described by the model except at  $p_T < 3$  GeV, while a disagreement is found with the statistical hadronization theory. The measurement with PbPb data shows no dependence on the number of participants, but points toward a strong dependence of  $R_{\Lambda_c/D^0}$  with rapidity.

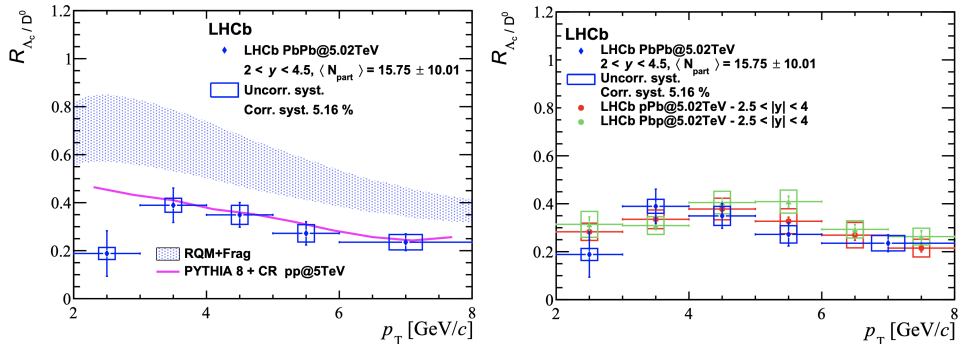


Fig. 1. Measurement of the  $\Lambda_c^+$ -to- $D^0$  ratio as a function of  $p_T$  compared to theoretical models (left) and to a previous LHCb measurement with  $p$ Pb data (right).

### 2.2. Coherent charmonium production in ultra-peripheral lead–lead collisions

In ultra-peripheral collisions (UPCs), the two ions interact via a photon–nuclear process. If the photon interacts with the whole nucleus coherently, this process is a great tool to constrain the gluon parton distribution function (PDF). Hence, the coherent  $J/\psi$  and  $\psi(2S)$  production cross sections in PbPb UPCs at  $\sqrt{s_{NN}} = 5.02$  TeV are studied as a function of  $p_T$  [5].

Once the particles are reconstructed, the differential cross sections are separately measured for  $J/\psi$  and  $\psi(2S)$  as a function of the rapidity and the transverse momentum in the c.m. system in the ranges of  $2.0 < y^* < 4.5$  and  $0 < p_T^* < 0.2$  GeV/ $c$ , respectively. The ratio of cross sections between the coherent  $\psi(2S)$  and  $J/\psi$  yields as a function of  $y^*$  is precisely determined for the first time in PbPb collisions at the LHC, finding compatibility with theoretical models.

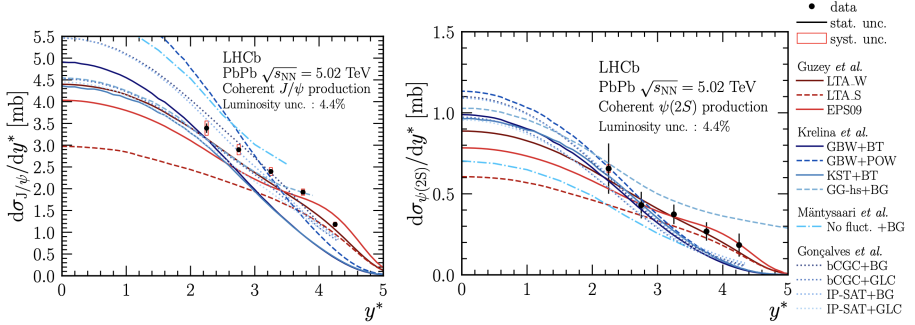


Fig. 2. (Colour on-line) Differential cross section as a function of  $y^*$  for coherent  $J/\psi$  (left) and  $\psi(2S)$  (right) production, compared to theoretical predictions. Models are grouped as perturbative QCD (red lines) calculations and colour glass condensate (blue lines).

### 3. Fixed-target collisions results

#### 3.1. $\bar{p}$ production from antihyperon decays in $pHe$ collisions at $\sqrt{s_{NN}} = 110$ GeV

The LHCb fixed-target programme is also relevant to cosmic ray physics, *e.g.* to constrain the flux of antiprotons in space originating in cosmic rays spallation on the interstellar medium, mainly composed of hydrogen and helium. The antiproton production has been measured in the  $pHe$  sample at  $\sqrt{s_{NN}} = 110$  GeV, an energy scale relevant for the AMS-02 measurements of antimatter in space [6, 7]. Prompt  $\bar{p}$  measurements already constrained models of secondary cosmic antiprotons [8]. Thus, searches are now extended to antiprotons produced by antihyperons decays performed with two complementary approaches: (i) inclusive measurements of detached antiprotons using impact parameter and  $\bar{p}$  identification; (ii) exclusive measurements of the dominant contribution  $\bar{\Lambda} \rightarrow \bar{p}\pi^+$ . Despite that the most commonly used hadronic models underestimate the antihyperon contributions to the total yield (Fig. 3 (left)), an agreement of the exclusive  $\bar{\Lambda}$  over inclusive antihyperon ratio  $R_{\bar{\Lambda}/\bar{H}}$  with theoretical expectations can be found (Fig. 3 (right)).

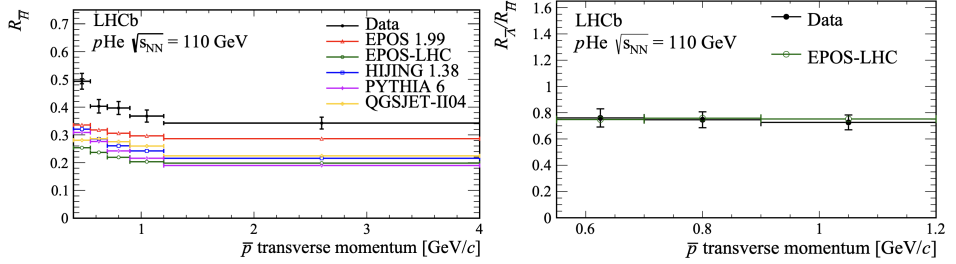


Fig. 3. Measurement of  $R_H$  ratio as a function of the transverse momentum compared to theoretical predictions (left); detached-to-prompt  $\Lambda$ -to- $H$  ratio with the EPOS-LHC prediction (right).

### 3.2. Charmonium production in $p\text{Ne}$ collisions at $\sqrt{s_{NN}} = 68.5$ GeV

Charmonia production is an excellent probe for Cold Nuclear Matter effects such as PDF nuclear modification, nuclear absorption, multiple scatterings, *etc.* The production of  $J/\psi$  and  $\psi(2S)$  mesons reported here is studied with 2.5 TeV protons colliding on gaseous neon targets at rest, corresponding to  $\sqrt{s_{NN}} = 68.5$  GeV [9]. The  $J/\psi$  differential cross section is in good agreement with predictions with and without 1% intrinsic charm contribution, while there is tension between data and HELAC-ONIA model (Fig. 4 (left)) [10]. This is the first measurement of the  $\psi(2S)$ -to- $J/\psi$  production ratio with SMOG, and it is consistent with other  $pA$  measurements at small atomic mass number  $A$  (Fig. 4 (right)), but with limited statistics. This suggests and motivates the fixed-target programme upgrade.

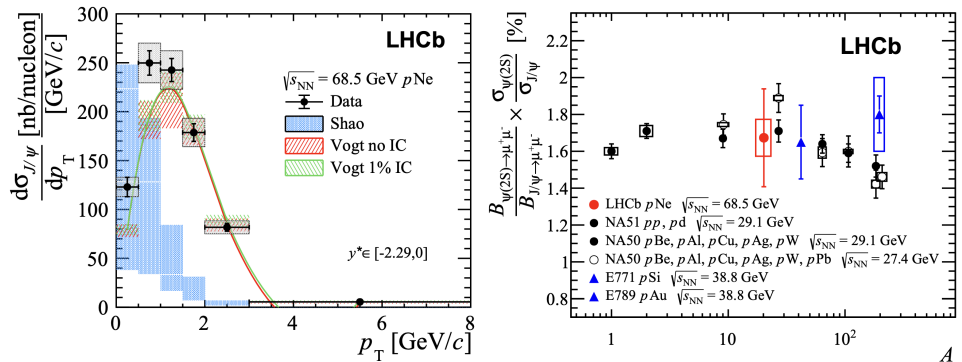


Fig. 4. (Colour on-line) Differential  $J/\psi$  cross section as a function of  $p_T$  (left). Blue boxes correspond to HELAC-ONIA predictions. Green and red boxes correspond to predictions (Vogt) with and without a 1% intrinsic charm contribution, respectively. The  $\psi(2S)$ -to- $J/\psi$  production ratio as a function of the target atomic mass number  $A$  (right).

### 3.3. $J/\psi$ and $D^0$ production in PbNe collisions at $\sqrt{s_{NN}} = 68.5$ GeV

At larger values compared to the QGP critical temperature ( $\sim 156$  MeV), lattice QCD predicts the charmonium production decrease with respect to the overall  $c\bar{c}$  production, due to the modification of their binding mechanism [10]. Consequently, since most of the charm quarks hadronize into open charm mesons, the  $D^0$  production yield provides a suitable reference for the study of the charmonium yield modification when traversing nuclear media. The production of  $J/\psi$  and  $D^0$  mesons is studied for the first time with a beam of lead ions with an energy of 2.5 TeV per nucleon colliding on gaseous neon targets at rest, corresponding to a nucleon–nucleon c.m. energy of  $\sqrt{s_{NN}} = 68.5$  GeV [11]. The  $J/\psi$  over  $D^0$  production cross section is computed as a function of rapidity, transverse momentum, and collision centrality. A decrease of  $J/\psi$  over  $D^0$  ratio with increasing centrality has been observed, in agreement with NA50-SPS  $pA$  measurements (Fig. 5 (left)) [12]. Hence, these data are compared with measurements from  $pNe$  collisions at the same energy. No anomalous  $J/\psi$  suppression that could indicate the formation of a deconfined medium is observed (Fig. 5 (right)).

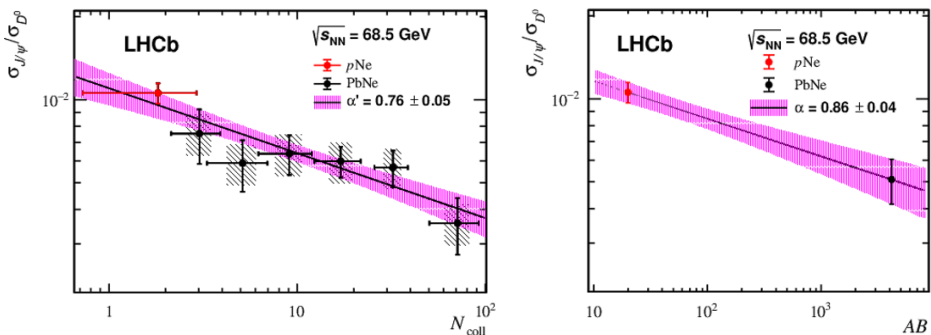


Fig. 5. (Colour on-line) Left:  $J/\psi/D^0$  cross-section ratio as a function of the number of binary collisions,  $N_{\text{coll}}$ . The red and black points correspond to  $pNe$  and  $PbNe$  collisions, respectively. Right:  $J/\psi/D^0$  cross-section ratio as a function of  $AB$ , the product of the beam (A) and target (B) atomic mass numbers.

## 4. Run 3 performance: the LHCb upgrade

The LHCb has undergone a major upgrade in 2018–2022 to meet the challenge of the increased luminosity in the LHC Run 3 [13]. The upgrade will reduce the occupancy limitation in PbPb collisions and allow for access to mid-central PbPb collisions up to 30% in centrality (Fig. 6 (left)). The other significant improvement is the new fixed-target storage cell located upstream of the LHCb interaction point, SMOG2 (Fig. 6 (right)). This new

configuration allows for the injection of heavier noble gases (Kr, Xe) and non-noble species ( $H_2$ ,  $D_2$ ,  $O_2$ ,  $N_2$ ) with a pressure of about two orders of magnitude higher than the SMOG one for the same gas flow, leading to higher luminosities for fixed-target collisions [14].

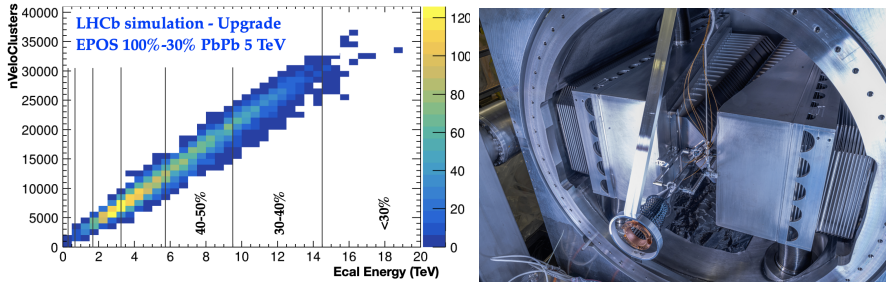


Fig. 6. Left: Reconstruction performance in LHCb Run 3 for Pb-Pb collisions. The nVeloClusters variable is related to the centrality. Right: SMOG2 storage cell.

## 5. Conclusions and outlook

The results presented here from PbPb datasets demonstrate the capabilities of LHCb in studying nuclear effects in different centrality regions. In addition, the fixed-target programme is relevant also to cosmic ray physics as well as nuclear matter effects and QGP formation.

With the upgrade, LHCb will be able to acquire PbPb and fixed-target data samples with increased statistics, opening the gates to more precise measurements and a wider variety of possible analyses. PbPb collisions up to mid-central events will enable QGP studies, and SMOG2 will bring the current fixed-target measurements to a new level.

## REFERENCES

- [1] LHCb Collaboration (A.A. Alves Jr. *et al.*), *J. Instrum.* **3**, S08005 (2008).
- [2] LHCb Collaboration (R. Aaij *et al.*), *Int. J. Mod. Phys. A* **30**, 1530022 (2015), [arXiv:1412.6352 \[hep-ex\]](#).
- [3] LHCb Collaboration (R. Aaij *et al.*), *J. High Energy Phys.* **2023**, 132 (2023), [arXiv:2210.06939 \[hep-ex\]](#).
- [4] LHCb Collaboration (R. Aaij *et al.*), *J. High Energy Phys.* **2019**, 102 (2019), [arXiv:1809.01404 \[hep-ex\]](#).
- [5] LHCb Collaboration (R. Aaij *et al.*), *J. High Energy Phys.* **2023**, 146 (2023), [arXiv:2206.08221 \[hep-ex\]](#).
- [6] LHCb Collaboration (R. Aaij *et al.*), *Eur. Phys. J. C* **83**, 543 (2023), [arXiv:2205.09009 \[hep-ex\]](#).

- [7] A. Kounine, *Int. J. Mod. Phys. E* **21**, 1230005 (2012).
- [8] LHCb Collaboration (R. Aaij *et al.*), *Phys. Rev. Lett.* **121**, 222001 (2018).
- [9] LHCb Collaboration (R. Aaij *et al.*), *Eur. Phys. J. C* **83**, 625 (2023),  
[arXiv:2211.11645 \[hep-ex\]](#).
- [10] H.-S. Shao, *Comput. Phys. Commun.* **198**, 238 (2016),  
[arXiv:1507.03435 \[hep-ph\]](#).
- [11] LHCb Collaboration (R. Aaij *et al.*), *Eur. Phys. J. C* **83**, 658 (2023),  
[arXiv:2211.11652 \[hep-ex\]](#).
- [12] NA50 Collaboration (M.C. Abreu *et al.*), *Phys. Lett. B* **410**, 337 (1997).
- [13] LHCb Collaboration, CERN-LHCC-2012-007; LHCb-TDR-012.
- [14] LHCb Collaboration, LHCb-TDR-020.